Pergamon

Engineering Failure Analysis, Vol. 5, No. 2, pp. 129–141, 1998

Printed in Great Britain
1350–6307/98 $19.00 + 0.00

PII: S1350–6307(98)00010–7

AUTOMOTIVE COMPONENT FAILURES

A. M. HEYES

Advanced Engineering and Testing Services, CSIR, Private Bag X28, Auckland Park 2006, Republic of South Africa.

(*Received* 3 *February* 1998)

Abstract—The failure of vehicle components is an area which is likely to affect all of us at one stage or another. In this paper the distribution of component failures is discussed, as well as the causes thereof. Four case studies are presented to give insight in the methodology of failure analysis of automotive components, and the valuable information which can be gained thereby. © 1998 Elsevier Science Ltd. All rights reserved.

Keywords: Accident investigation, automotive failures, decarburization, fatigue, weld fatigue.

1. INTRODUCTION

Failure of automotive components is an occurrence which affects the life of almost every person at one stage or another. Components in a vehicle often operate under arduous conditions and in many cases are required to last the lifetime of the vehicle without any form of inspection. Often, the failure of a component results in no more than a nuisance with replacement of that part being required. However, failure of some components can result in loss of control of the vehicle, with the obvious possibility of accidents and loss of life. Such parts are known as *safety critical items* and a batch related in-service failure of such parts will often result in the recall of all affected vehicles with the associated cost and bad publicity. Thus, it is often the case in automotive failure analysis that it is imperative to determine whether the failure is an isolated case or is likely to occur in more vehicles.

Based on an analysis of seventy automotive component failures received for investigation the distribution of component failure and the distribution of causes are given in Figs 1 and 2 respectively. From this it can be seen that the most common component failure is that of the engine (41%) and that the most common cause of failure is abuse (29%). However, the total contribution to the cause of failure of manufacturing or design errors, raw material defects and or storage procedures is 33%. It can also be argued that as cars are being kept longer, partly due to economic pressures and partly due to improvements in chassis technology, the other components should be designed for a longer lifetime. The inclusion of age related failures as a manufacturing responsibility increases this figure to 43%. This represents a significant area for improvement on the part of the manufacturers. By the same token, the high proportion of failures due to failed repairs (18%) represents an area where increased training in the reconditioning and refurbishing industry may yield significant dividends.

This paper presents four summarised case studies of automotive component failures, with the aim of demonstrating the valuable information which can be gained by failure analysis.

2. CASE STUDY 1—MANUFACTURING DEFECT

2.1. *Background*

Complaints were received by a manufacturer that some of the new model vehicles that they had sold were producing oil smoke. While it was initially thought by the manufacturer that the smoking was related to the running-in period of the engines, it was found that the smoking did not disappear once the engines had been run-in. Stripping of the engines had not shown any evident source of oil

* Author to whom correspondence should be addressed.

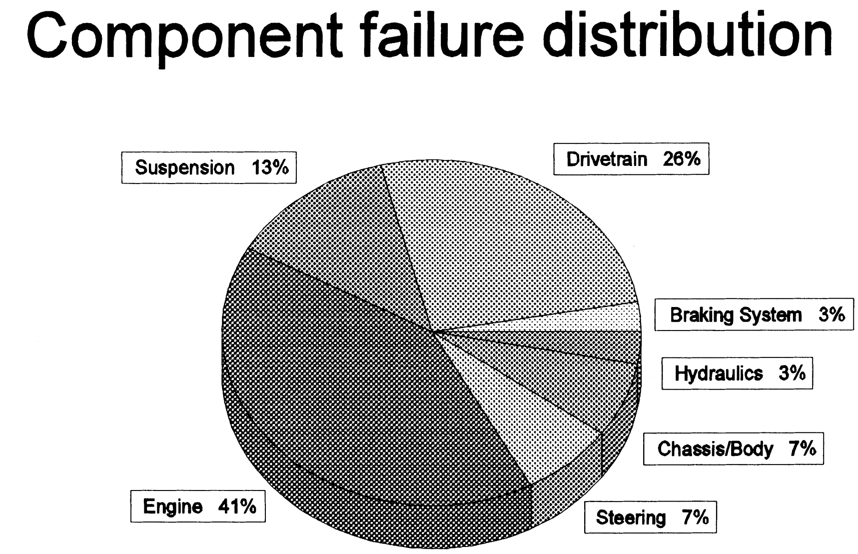

Fig. 1. The distribution of component failures.

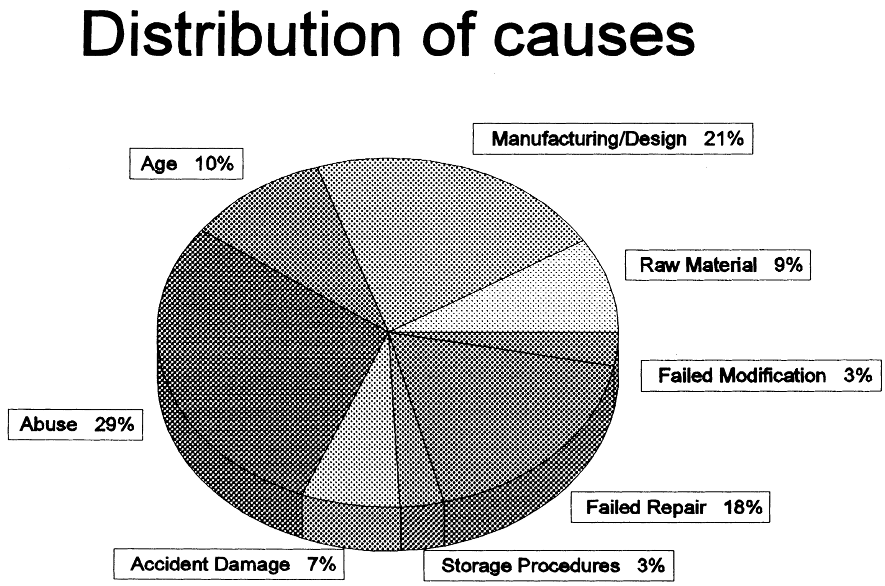

Fig. 2. The distribution of causes of failure.

ingress. An engine which had been removed from a vehicle due to smoking was supplied for investigation. The engine had been in service for approximately 20,000 km.

2.2. *Visual examination*

Upon stripping the engine it was found that one of the combustion chambers showed heavy carbonaceous deposits indicative of the burning of oil (Fig. 3) Circumferential black marks were found at differing heights in the bores of three of the cylinders. The visible honing pattern was deemed to be satisfactory. No source of oil ingress was evident at this stage.

2.3. *Dimensional measurements*

Measurements of the ovality and taper of the bores and the ring gaps all gave good results. This, together with the satisfactory honing pattern, made leakage of oil past the rings unlikely.

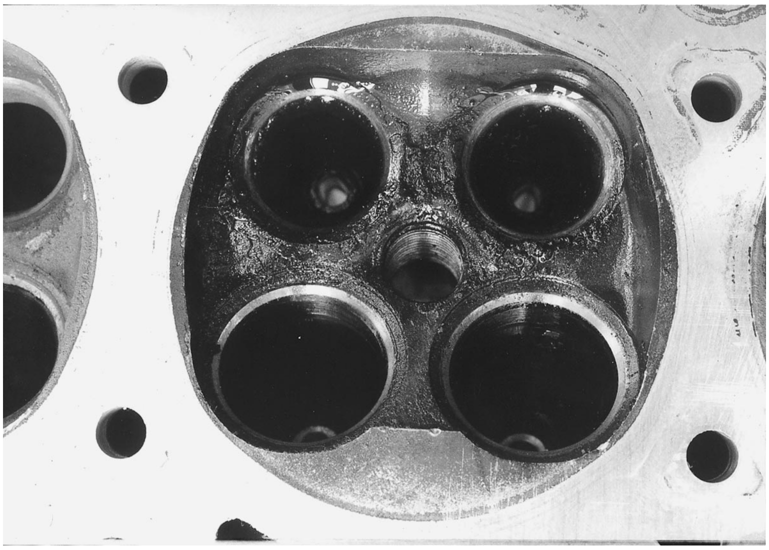

Fig. 3. Carbonaceous deposits left in combustion chamber by burnt oil.

Measurement of the flatness of the sealing face of the aluminium head and the deck of the block showed only negligible (0.05 mm) deviation from flatness and, as the head gasket showed no signs of leakage, ingress of oil via the head to block seal was ruled out.

2.4. *Magnetic particle inspection* (*MPI*)

The circumferential mark in the affected cylinder was indicated by MPI as being a crack like defect. However, upon sectioning the cylinder bore it was found that the marks were, in fact, shallow corrosion and fretting marks left where the chromium plated piston rings contacted the cylinder wall. The presence of these marks is explained by the fact that the engines are imported and are test run before shipping, quite possibly leaving combustion condensate in the cylinder. It was possible to eliminate these as a cause of oil ingress as they did not penetrate the cylinder wall and were not deep enough to retain significant amounts of oil.

2.5. *Fluorescent dye penetrant inspection and leak testing of cylinder head*

Due to the non-magnetic nature of the cylinder head fluorescent dye penetrant testing was carried out but failed to show any significant defects in the head. An alternate testing procedure involving pressurisation of the inlet ports and immersion of the head in a water bath showed the source of oil ingress to be a crack in the head where the valve guide had been inserted (Fig. 4). Fluorescent dye penetrant testing had failed to show the defect as it had been hidden under a steel spring seat.

2.6. *Conclusions*

This crack led through to the inlet port of the affected cylinder and the engine would draw oil into the engine on every intake stroke. Inspection of the inlet ports of other affected engines showed the same defect. The cause of the defect was related to manufacturing tolerances where the interference fit of the valve guide and the head was too tight, resulting in cracking of the head adjacent to the guide.

3. CASE STUDY 2—RAW MATERIAL DEFECT IN TORSION BAR

3.1. *Background*

Torsion bars are used in the suspension of some vehicles, either to replace conventional springs or to form part of anti-sway system. As the handling of a vehicle is drastically affected by a failure in either role, torsion bars fall into the category of safety critical items, as discussed in Section 1.

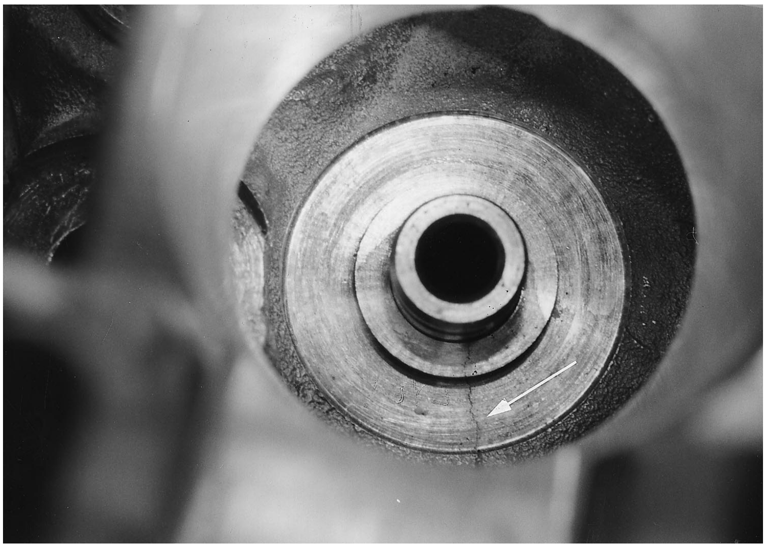

Fig. 4. The crack in the cylinder head caused by insertion of the valve guide.

In this case a torsion bar failed after completing 100,000 km service and was submitted for investigation by the vehicle manufacturer. It was required that the cause of failure be determined and also whether failures in other vehicles could be expected.

3.2. *Visual and stereo microscope examination*

The section of torsion bar submitted for examination was coated with a black paint coating which had flaked off at localised spots, where light rusting had occurred. The fracture surface (Fig. 5) showed the spiral shape typical of a tensile-type torsional failure [1], and the fracture surface appeared brittle in nature. Chevron markings clearly pointed to the fracture origin being some form of longitudinal defect.

After removal of the coating by means of trichloroethylene vapour bath, the bar was again visually examined but did not show any further significant details.

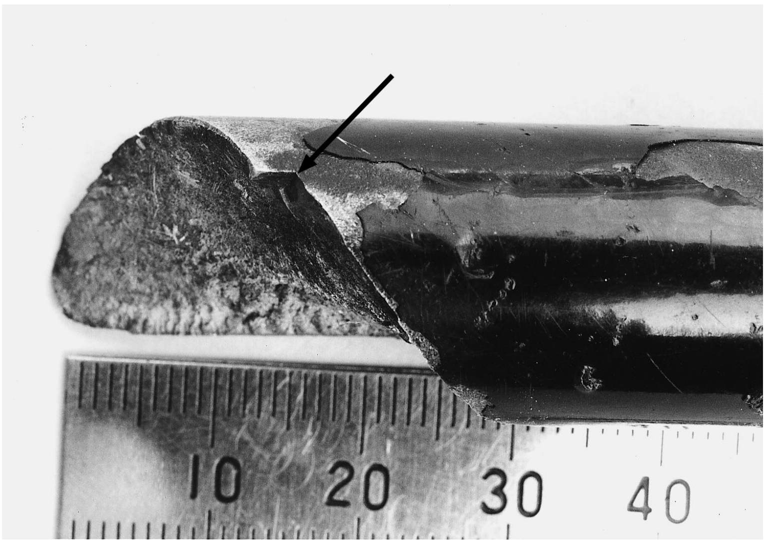

Fig. 5. Torsional failure of the bar, showing the likely fracture origin to be a longitudinal defect (arrowed).

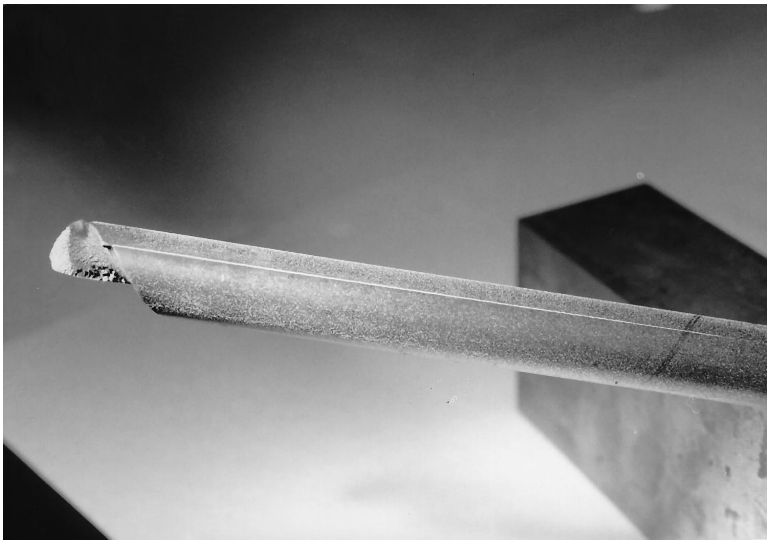

Fig. 6. Seam defect in torsion bar highlighted by fluorescent MPI.

3.3. *Fluorescent magnetic particle inspection*

Fluorescent magnetic particle inspection showed that a seam or lap defect existed for a further 200 mm from the fracture site (Fig. 6). Such defects are usually laps formed by incorrect rolling procedures or are seams attributable to steel defects (inclusions). Two further seams were found, but were of a very small size.

3.4. *Chemical analysis*

The bar was found to be a chromium steel meeting the compositional requirements of an AISI 5150 steel (0.53% C, 0.82% Mn, 0.81% Cr). This composition would indicate a high hardenability steel.

3.5. *Hardness testing*

Hardness tests gave a hardness of 508 HV30 which equates to an ultimate tensile strength of approximately 1740 MPa [2]. Such high tensile strengths are required to prevent yielding or fatigue of the bar during operation. A disadvantage of steels which rely on non-toughening strengthening additions such as carbon, manganese and chromium is that strength and toughness are inversely related, i.e. high strength levels result in low toughness.

3.6. *Scanning Electron Microscope (SEM) fractographic examination*

The fracture surface was sectioned from the remainder of the bar and was examined in the SEM. Figure 7 clearly shows how a penny shaped fatigue crack had grown from the seam defect. When the crack had grown to a size of approximately 3.5 mm the bar was unable to tolerate a defect of this size and underwent fast fracture. This relatively small defect tolerance is related to the low toughness, as described above. Figure 8 shows the appearance of the area of fatigue crack at 2000 times magnification. The morphology of the surface is typical of a steel fatigue fracture surface. Higher magnification examination of the fracture surface failed to show individual striations, this being usual for high strength steels.

The presence of a stress concentrating factor such as a crack can often change the torsional fracture mode from one of shear to tensile fracture (as in this case). This is due to the relationship between ultimate shear stress and ultimate tensile stress. In the case of steels where the ultimate shear stress is approximately half of the ultimate tensile stress, a shear failure would be expected.

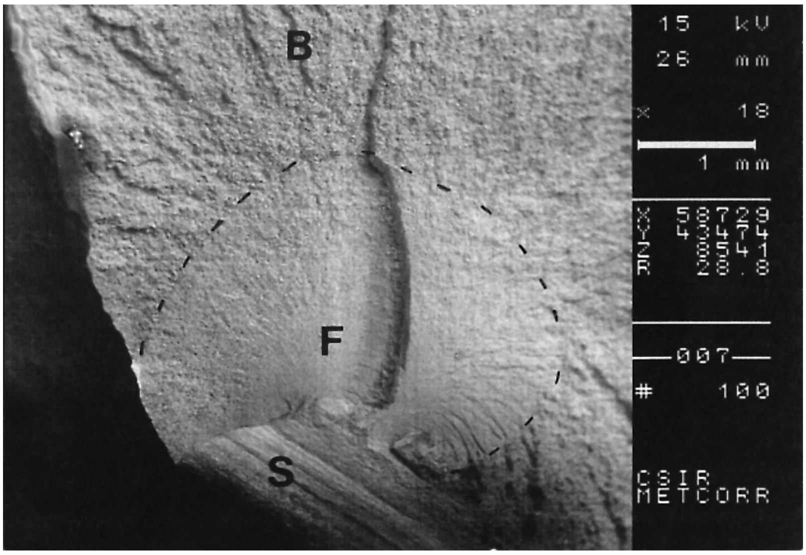

Fig. 7. Low magnification fractograph showing the seam defect (**S**), fatigue area (**F**) and the brittle fracture area (**B**).

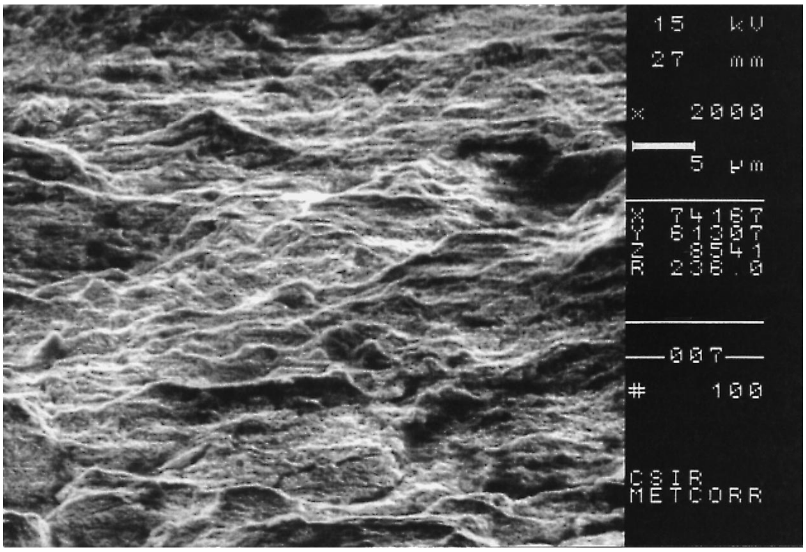

Fig. 8. Fracture surface marked **F** in Fig. 7, typical of a fatigue fracture surface in a high strength steel.

However, in the presence of a stress concentration the ultimate tensile stress can be exceeded before the ultimate shear stress is reached, resulting in a tensile failure [1].

3.7. *Metallography and Energy Dispersive Spectroscopy* (*EDS*)

A microspecimen was prepared from a transverse section taken adjacent to the fracture. An initial examination under an optical microscope showed a seam defect of depth 1.22 mm that was associated with numerous inclusions along the flanks of the defect. To allow for a more detailed analysis of the defect, including EDS, the specimen was examined in the SEM.

Figure 9 shows an SEM micrograph of the seam, together with a higher magnification micrograph of a selected area. The inclusions are clearly visible in the higher magnification micrograph. It was noted that the inclusions were only found to a depth of 0.84 mm. A high magnification micrograph of the seam and inclusions is given as Fig. 10.

To assist in identifying the inclusions EDS mapping of the area shown in Fig. 10 was carried out.

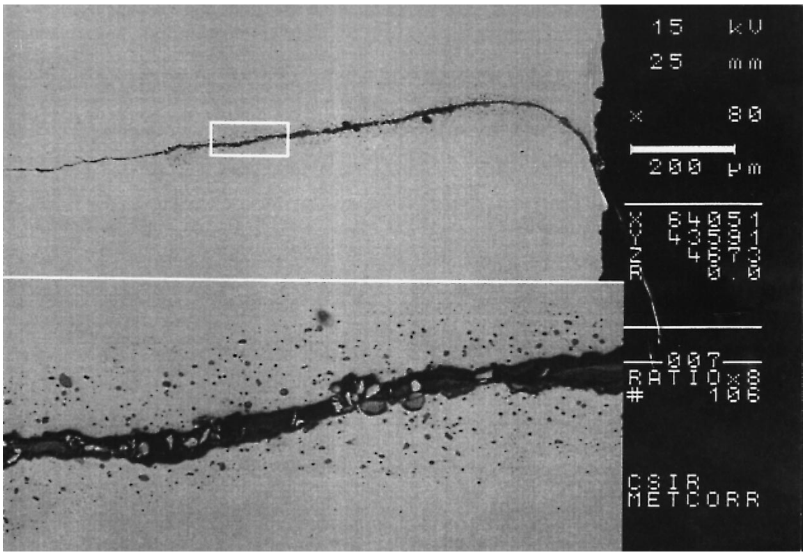

Fig. 9. SEM micrograph of seam (unetched). Note that the inclusions extend only to a depth of 0.84 mm.

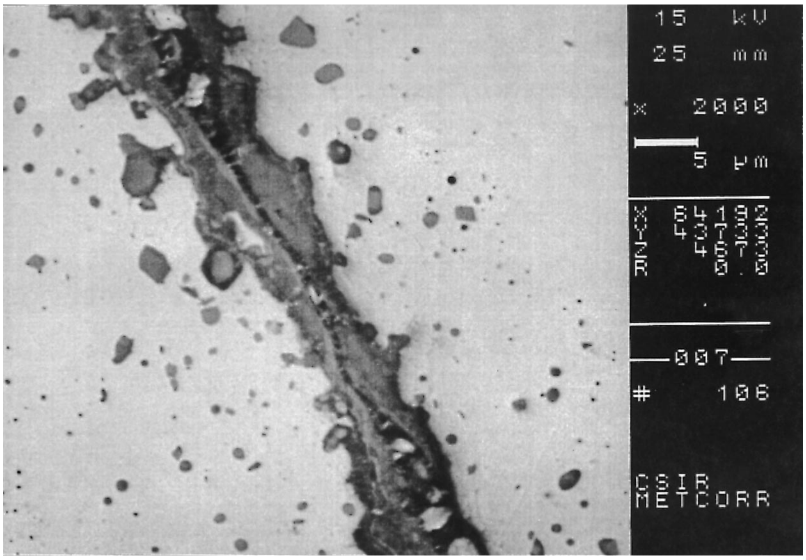

Fig. 10. SEM micrograph of the seam and surrounding inclusions (unetched).

The elements selected for mapping were determined by spot analysis of four random inclusions. The EDS map is shown as Fig. 11, where it can be seen that the seam is filled with iron oxide and that the discrete inclusions contain silicon, oxygen, chromium and manganese. Further EDS spot analysis indicated that the inclusions were probably a mixture of manganese iron silicate and chromite.

Etching of the microstructure in a 2% Nital etchant showed a decarburized area along the flanks of the seam (Fig. 12). It was noted that this extended to the depth of the inclusions, i.e. 0.84 mm. This implies that the defect was formed during the hot rolling operation of steelmaking. While the bar undoubtedly undergoes a quench and temper heat treatment, the only place for such cracking to occur during heat treatment would be in the quench cycle. This would be followed by tempering at temperatures unlikely to result in the observed decarburization. It should also be noted that high temperature oxidation accounts for the iron oxide (mainly FeO and Fe_3O_4) found within the crack. It can also be inferred, from the depth of the decarburization, that the seam defect grew somewhat after its formation.

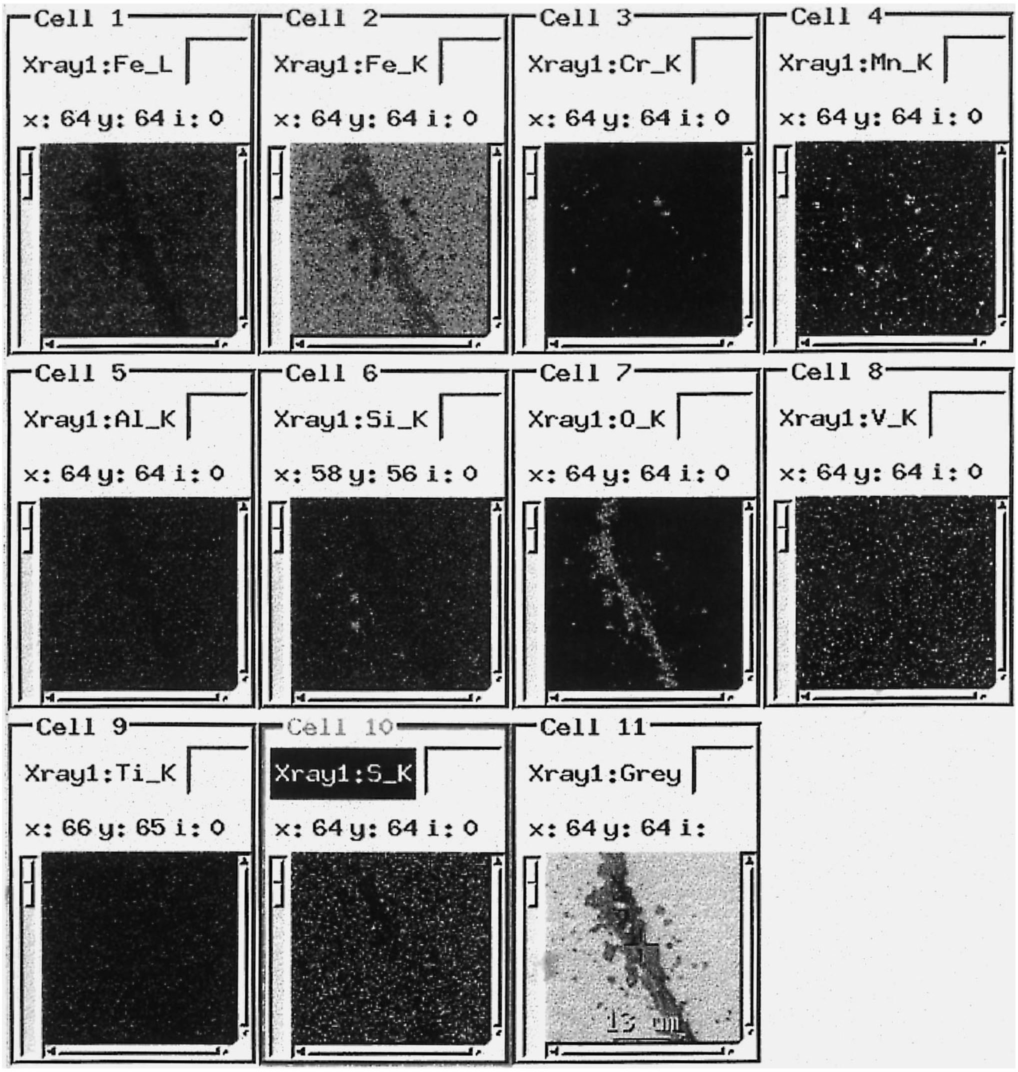

Fig. 11. Energy Dispersive Spectroscopy (EDS) map of the area shown in Fig. 9.

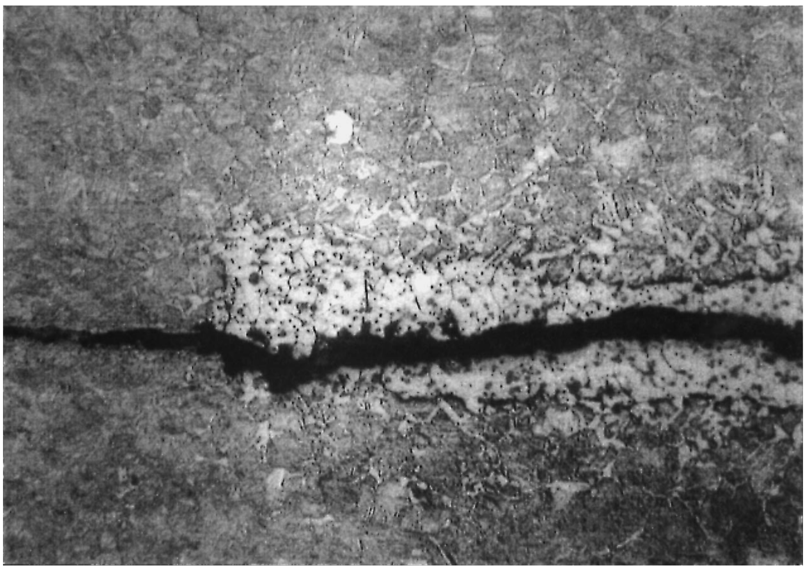
Fig. 12. Decarburization along the seam flanks, indicating high temperature oxidation (etched in 2% Nital).

3.8. *Conclusions*

The failure of the torsion bar occurred due to the growth of a small fatigue crack from a seam defect. Once the fatigue crack had reached a critical size, the bar failed by brittle fracture.

It was determined that the seam defect was caused by the presence of a segregated mixture of manganese iron silicate and chromite inclusions, the presence of which is related to a problem in the steelmaking process. These inclusions probably caused the bar to split during hot rolling, as evidenced by the decarburization of the flanks of the seam.

As the failure was related to a steelmaking problem it is likely to affect more than one vehicle. It was therefore recommended that the torsion bars of affected vehicles (i.e. manufactured from that particular cast of steel) be replaced. An audit of the non-destructive testing procedures of the component supplier was also recommended, as the defect was easily detectable by standard non-destructive techniques.

4. CASE STUDY 3—FAILED PASSENGER VEHICLE DRIVESHAFT

4.1. *Background*

Driveshafts comprising two constant velocity (CV) joints and the actual shaft are almost universally used in front wheel drive (FWD) vehicles to transmit power from the gearbox to the driven wheels. Although variations in form, i.e. solid or tubular, and type of material do occur, most are of the solid steel bar variety (which could also be considered a torsion bar.) Usually a vibration damper is attached at some point along the longer of the two driveshafts.

In this particular case study a driveshaft from an FWD hatchback was submitted for examination after failure, which resulted in the car suddenly pulling right and crashing into a stormwater drain. Significant impact damage was caused to the vehicle. When the vehicle was repaired it was found that the driveshaft had broken close to the wheel hub. The vehicle was used as a delivery vehicle for a small company and had numerous drivers, but was lightly loaded as it was used only to deliver foodstuffs. The vehicle was reported to be approximately two years old.

4.2. *Visual and stereo microscope examination*

The section of driveshaft received for analysis measured approximately 60 cm in length and had failed just after a gradual change in section. Close examination of the fractured end of the shaft showed evident scoring (Fig. 13), with light blue interference film oxides visible in this region.

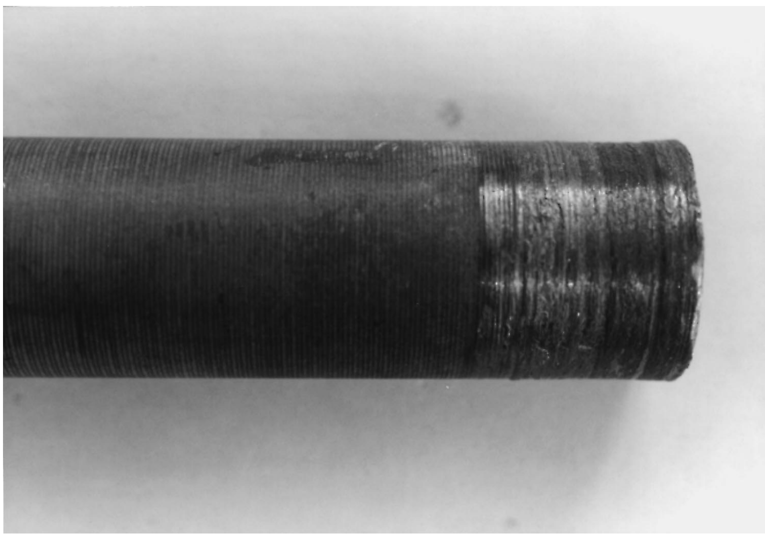

Fig. 13. The fractured end of the driveshaft. Note the scoring.

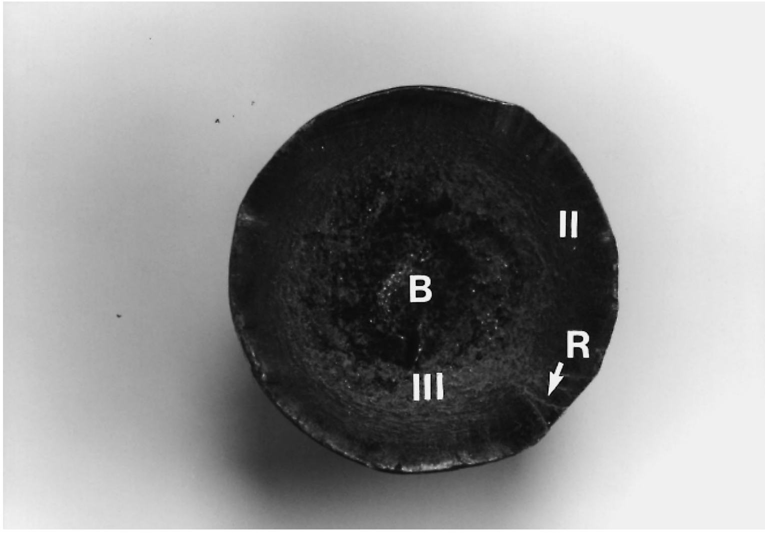

Fig. 14. Fracture surface of the driveshaft, showing a fatigue induced failure. (**R**—ratchet marks, **II**—Stage II fatigue growth, **III**—Stage III fatigue growth, **F**—fast fracture).

Measurement of the scored regions on both pieces of driveshaft showed the scoring to be approximately 30 mm wide.

The fracture surface is shown in the as-received condition in Fig. 14, where the failure can be seen to be due to rotating bending fatigue. In such cases, numerous circumferential cracks initiate and grow together to form one circumferential crack front, giving rise to the ratchet markings observed on this fracture surface. As the crack grows (stage II fatigue crack growth) the stress intensity range (ΔK) driving the fatigue crack growth increases. This leads to a transition from stage II to stage III crack growth, evidenced by the increasing roughness of the fatigue fracture surface towards the centre of the driveshaft. At some point the increasing crack length results in a maximum strength intensity (K_{max}) greater than the fracture toughness of the material (K_c) and fast fracture occurs. It was estimated that only 42% of the cross-sectional area remained when fast fracture occurred, showing that the shaft had a significant safety factor against fast fracture.

4.3. *Microscopic examination*

Components such as driveshafts generally show a fatigue lifetime much greater than the lifetime of the vehicle. This indicates that the fatigue process is dominated by the crack initiation process rather than the crack propagation process. Failure of such components is therefore related to either abnormally high stresses, a reduction in material strength which eases the initiation of fatigue cracks (e.g. decarburization) or to some form of defect which eliminates the crack initiation stage.

In this case the scoring of the surface of the driveshaft has effectively eliminated the initiation phase of the fatigue cracking process. Figure 15 shows a micrograph of a longitudinal section taken through the scored section of driveshaft. Numerous fatigue cracks can be seen to emanate from the scoring.

4.4. *Conclusions*

The fatigue cracking of the driveshaft was found to have initiated due to scoring of the surface. Upon inspection of the vehicle it was found that there was an indent, of a size corresponding to the diameter of the driveshaft, in the vertical chassis member near the wheel hub. The chassis member was also approximately 30 mm in width, the same width as the scored region on the driveshaft. Evidently, the rotating driveshaft had contacted the chassis at some stage, resulting in the observed scoring.

It was found that under normal conditions, the driveshaft was displaced from the vertical chassis member by a distance of 15 mm and that it would require a substantial load on the suspension to

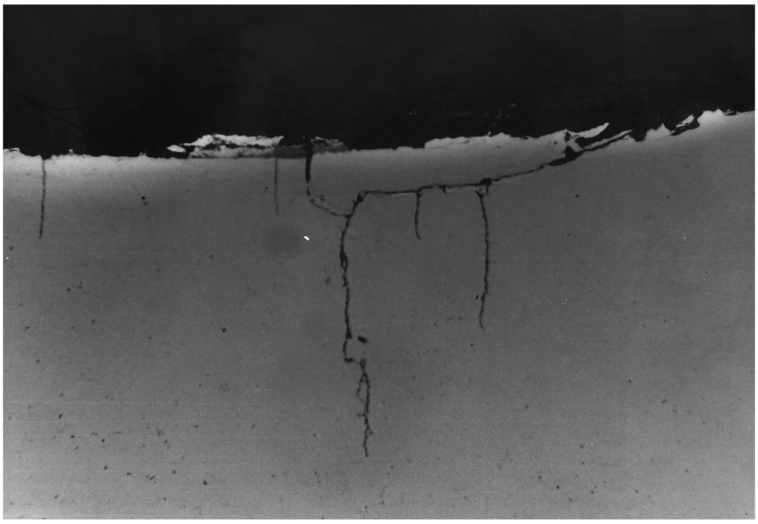

Fig. 15. Longitudinal micrograph taken through scored region of driveshaft (unetched).

force the driveshaft into contact with the chassis. It would, therefore, appear that the vehicle had been involved in some accident prior to the one resulting from the failure of the driveshaft.

This case study highlights the fact that what may look to the unpractised eye to be insignificant damage can easily lead to the long term failure of such components. In this case it is quite possible that the scoring of the driveshaft was observed at an earlier stage but was judged by the person carrying out the repair to be superficial damage.

5. CASE STUDY 4—FAILED CRANKSHAFT REFURBISHMENT

5.1. *Background*

Crankshafts from industrial engines (usually diesel engines) are occasionally damaged by lubrication or bearing failures or simply wear below acceptable limits due to extended use. The manufacturers' recommendation in such cases is to install a new crankshaft. However, many owners balk at the expense of a new crankshaft and opt to have the damaged crankshaft refurbished. This process usually involves welding onto the surface of the journals to build them up to oversize and then grinding down to the original, correct journal size.

This case study involves the failure analysis of a refurbished diesel engine crankshaft.

5.2. *Visual examination*

Figure 16 shows the section of crankshaft received for failure analysis. It can be seen that the failure has occurred at the second big end journal.

In this case the cause of the failure could be determined with no more than a visual inspection and low power microscopy. The fracture surface of the journal showed evidence of fatigue, with two opposed fatigue cracks and a very small fast fracture area. One of the cracks grew to a depth of 75% of the diameter of the journal. Figure 17 shows a close up view of the large fatigue fracture surface with beach markings clearly evident. Weld build up is also visible, evidenced by its scalloped appearance on the fracture near the journal surface. This showed that the crankshaft had been refurbished.

The origin of the fatigue crack is evidently the oil hole, which can be seen to have been poorly drilled out following weld build up of the journal. Inspection of the other oil holes showed another hole to have been poorly dressed, leaving a sharp notch at the intersection of the oil hole and the journal surface.

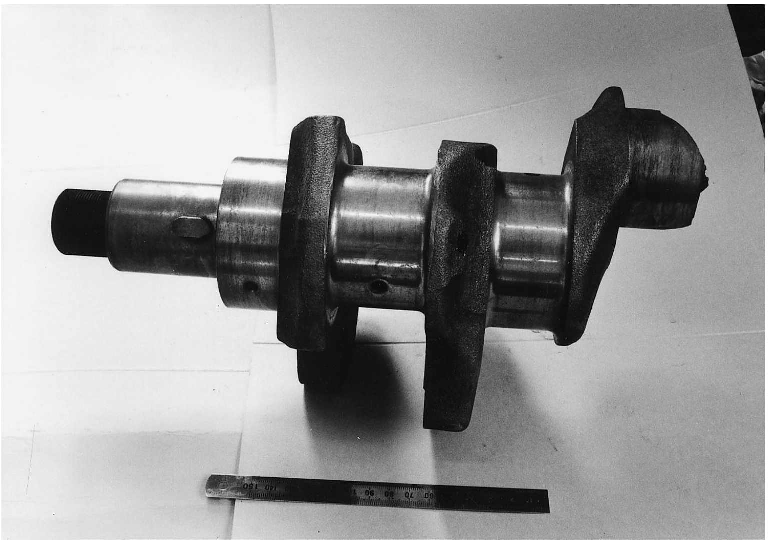

Fig. 16. The as-received section of crankshaft.

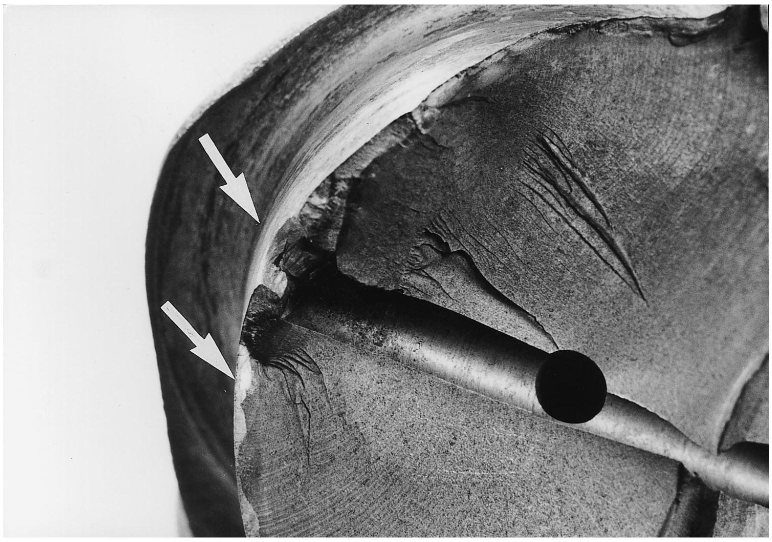

Fig. 17. The fracture surface of the journal showing clear beach markings, indicative of fatigue. The fatigue crack initiated at the mismatched oil hole. Note the scalloped appearance of the weld deposit near the surface of the journal.

5.3. *Conclusions*

The failure of the crankshaft was due to poor refurbishment of the journals by welding. The original oil hole and the drilled out hole were grossly mismatched creating a step of weld material. Fatigue cracking, probably initiated by cracking of the weld deposit at the oil hole, caused the crankshaft to fracture.

This case study highlights the need for expert knowledge when it comes to the refurbishment of crankshafts. Factors to be considered in refurbishing a crankshaft include machining tolerances, material of construction of the crankshaft, the process used to build up the journal diameter and the possible presence of surface treatments such as tufftriding, induction hardening or shot peening.

6. CONCLUSIONS

A review of the types and causes of automotive component failures has shown that while failures resulting from abuse and such like are unavoidable, there is the possibility for a substantial reduction in automotive component failures. The following are seen as possible areas for attention:

(1) Increased quality checks on the raw materials used to manufacture safety critical items.
(2) Improved assembly procedures during manufacture.
(3) Stricter control on the quality of refurbishment and improved training of those doing the refurbishment.
(4) Education of the public as to the possibility of long term failures arising from what may appear to be minor damage or abuse.

The presented case studies have shown examples of in-service failures which highlight the above points. Also, the involvement of fatigue cracking in three out of four case studies shows that this is an important failure mechanism in automotive failures, as has been noted for general engineering failures [3].

Acknowledgement—The assistance of the staff at the Cottesloe laboratories in the examination of the discussed components is gratefully acknowledged.

REFERENCES

1. Avner, S. H., *Introduction to Physical Metallurgy*, 2nd ed. McGraw-Hill, 1974, pp. 660–662.
2. *ASTM Standard A*370, Table 2A, ASTM, 1995.
3. Hertzberg, R. W., *Deformation and Fracture Mechanics of Engineering Materials*, 3rd ed., John Wiley and Sons, 1989, pp. 457.